# Stable Stationary Solitons of the One-Dimensional Modified Complex Ginzburg-Landau Equation

Woo-Pyo Hong

Department of Electronics Engineering, Catholic University of Daegu, Hayang, Gyongsan, Gyungbuk 712-702, South Korea

Reprint requests to W.-P. H.; E-mail: wphong@cu.ac.kr

Z. Naturforsch. **62a,** 368 – 372 (2007); received May 14, 2007

We report on the existence of a new family of stable stationary solitons of the one-dimensional modified complex Ginzburg-Landau equation. By applying the paraxial ray approximation, we obtain the relation between the width and the peak amplitude of the stationary soliton in terms of the model parameters. We verify the analytical results by direct numerical simulations and show the stability of the stationary solitons. – PACS numbers: 42.65.Tg, 42.81Dp, 42.65Sf.

*Key words:* One-Dimensional Modified Complex Ginzburg-Landau Equation; Existence Condition of Stationary Solitons; Numerical Simulation.

The one-dimensional (1D) complex Ginzburg-Landau equation (CGLE) is one of the widely studied nonlinear equations for describing dissipative systems above the point of bifurcation [1]. The CGLE and its extension model a large variety of dissipative physical systems, such as binary fluid convection [2], electro-convection in nematic liquid crystals [3], patterns near electrodes in gas discharges [4], and oscillatory chemical reactions [5]. The continuous 1D CGLE possesses a rich variety of solutions including coherent structures such as pulses (solitary waves), fronts (shock waves), sinks (propagating holes with negative asymptotic group velocity), sources (propagating holes with positive asymptotic group velocity), periodic unbounded solutions, vacuum, periodic and quasi-periodic solutions, slowly varying fully nonlinear solutions, and a transition to chaos. However, there are many models which contain some small additional terms for various applications. As such an interesting example, we consider the 1D modified complex Ginzburg-Landau equation (MCGLE) which contains additional nonlinear gradient terms, in the form

$$\mathrm{i}\psi_t + p\psi_{xx} + q|\psi|^2\psi = c\frac{\psi_x\psi_x^*}{\psi^*} \qquad (1)$$

$$+ d\left[\frac{1}{2}(\psi\psi^*)_{xx}\psi\psi^* - \frac{1}{4}((\psi\psi^*)_x)^2\right]\frac{1}{\psi\psi^{*2}} + \mathrm{i}\gamma\psi,$$

where the parameters $p$, $q$, $c$, $d$ are taken as real constants, $\gamma$ is purely imaginary, and $\psi(x,t)$ is the complex wave function. The subscripts $t$ and $x$ denote the partial derivatives, and the asterisk indicates complex conjugation. The equation has been used to model collective motion on top of a superfluid covariant non-dissipative chaotic background if one considers possible vacuum dissipative effects [6, 7].

Recently, Yomba and Kofané [8] have found many different types of solution of (1) for the cases of complex $p$, $q$, $c$, $r$, and $d$. With a combination of the Painlevé analysis and Hirota's technique of bilinearizations they have found pulses, fronts, periodic unbounded waves, sources, and sink solutions. The purpose of the present work is to present the existence of a new family of stationary or non-traveling solitons by adopting the paraxial ray approximation method [9, 10] which has been used to find stationary solitons in photorefractive materials [11, 12]. We identify the regions of existence of these stationary solitons and reveal some of their interesting properties. Finally, we perform numerical simulations to show that the solitons are dynamically stable during their propagations which supports the paraxial ray approximation. In the rest of the paper, we consider the cases of real parameters $p$, $q$, $c$, $d$, and ignore the gain or loss term $\gamma$.

According to the paraxial theory of Akhmanov et al. [9], an optical beam or pattern preserves its structural form while propagating through the medium, i. e., the solution shows self-similar behaviour. This simple method can be applied to some non-integrable equations to find initial profiles which preserve self-similar

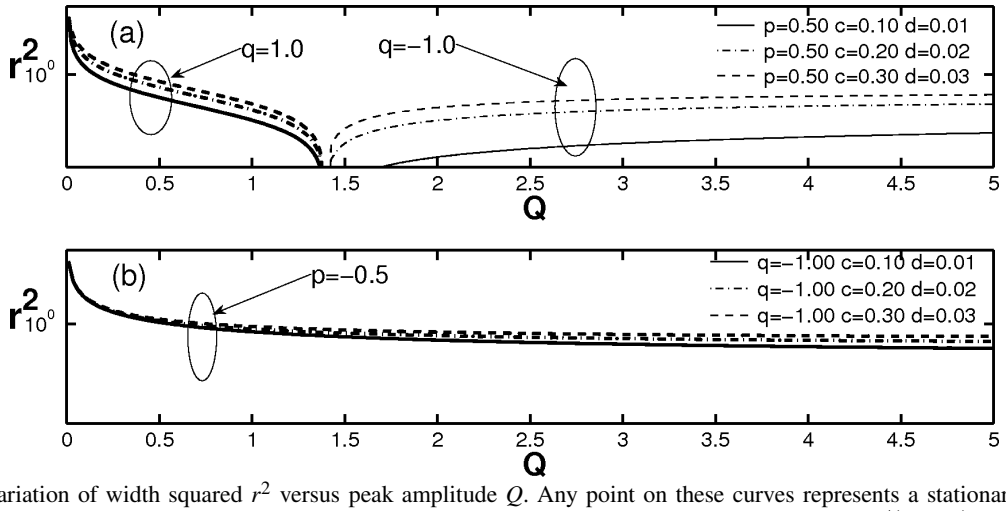


Fig. 1. Variation of width squared $r^2$ versus peak amplitude $Q$. Any point on these curves represents a stationary soliton. (a) For $q = 1.0$, the width rapidly decreases as both $c$ and $d$ increase for $Q$ in the range of $0 < Q < p/(c+2d)$. For $q = -1$, the width increases as both $c$ and $d$ increase and it saturates to a finite value as $Q >> p/(c+2d)$. (b) For $q = -0.5$, the width decreases as $Q$ increases regardless of the magnitude of the parameters.

behaviour [11, 12]. However, since the theory is not exact, its predictions need to be verified by detailed numerical simulations. In the following analysis, we look for a solution in the form of

$$\psi = A(x,t)\exp[-\mathrm{i}\Omega(x,t)]. \tag{2}$$

We substitute this into (1) and obtain

$$\begin{aligned} &A\Omega_t + p(A_{xx} - A{\Omega_x}^2) + qA^3 - c({A_x}^2 + A^2{\Omega_x}^2)A \\ &\quad - \frac{d[({A_x}^2 + AA_{xx})A^2 - A^2{A_x}^2]}{A} = 0, \end{aligned} \tag{3}$$

$$A_t + p(-2A_x\Omega_x - A\Omega_{xx}) - \gamma A = 0. \tag{4}$$

We further assume that the lowest-order localized bright soliton, for which the envelope is confined in the central region of the soliton, is $A(x=0,t)_{\max} = Q$, $A(x,t) = 0$ as $|x| \to \infty$, and the wave solution maintains its self-similar character while it propagates [11, 12]. Hence, the ansatz solution of the above equation can be written as

$$\begin{aligned} A(x,t) &= \sqrt{\frac{Q}{f(t)}}\exp\left[-\frac{x^2}{2r^2f^2(t)}\right], \\ \Omega(x,t) &= \frac{x^2}{2}\frac{\mathrm{d}\ln f(t)}{\mathrm{d}t}, \end{aligned} \tag{5}$$

where $Q$ is the peak amplitude at $x = 0$ and $f(t)$ is the variable pulse width parameter so that $rf(t)$ is the width of the soliton. We show in the following that the pulse radius $r$ can be found as functions of the system parameters. For a non-diverging soliton at $t = 0$, we set $f = 1$ and $\mathrm{d}f(t)/\mathrm{d}t = 0$. Substituting (5) into (3), since it only contains the differential terms of the amplitude of $A$, using the paraxial approximation [10–12], Taylor-expanding it with respect to $x$, and equating the coefficients of $x^2$ of (3), we obtain

$$\frac{\mathrm{d}^2f(t)}{\mathrm{d}t^2} = \frac{4p}{r^4f(t)^3} - \frac{4qQ}{r^2f(t)^2} - \frac{(8d+4c)Q}{r^4f(t)^4}. \tag{6}$$

Since we are interested in a non-singular bright soliton, we first look for the equilibrium point of the ordinary differential equation, which can be obtained by setting the left-hand side of (6) to zero, thus

$$r^2 = -\frac{c}{q} + \frac{p-2dQ}{qQ}, \tag{7}$$

which gives the relation between the width $r$, the system parameters, and the peak amplitude $Q$. To have a physically valid width, i. e., $r^2 > 0$, $Q$ should satisfy the constraints

$$\begin{aligned} &0 < Q < \frac{p}{c+2d}, \text{ if } q > 0, \\ &0 < \frac{p}{c+2d} < Q, \text{ if } q < 0. \end{aligned} \tag{8}$$

Figure 1a shows the existence curves of $(r^2, Q)$ in terms of different model parameters. Each point on

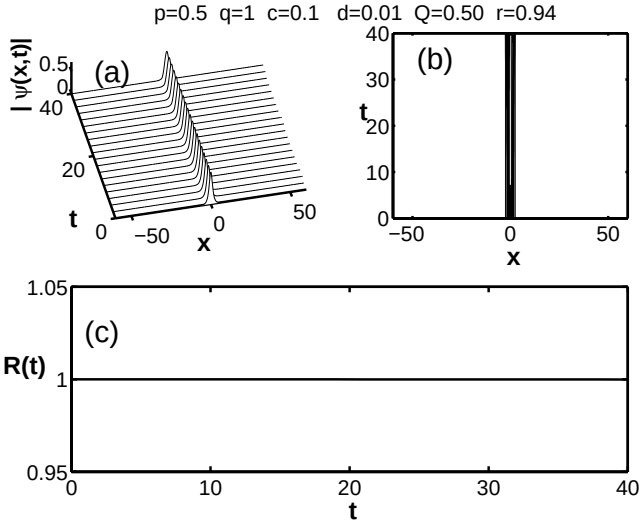


Fig. 2. (a) Numerically simulated propagation of a stationary soliton. The stable propagation confirms the analytical result obtained by the paraxial ray approximation. (b) Contour plot of (a). (c) Normalized energy $R(t)$ versus time. The constant value $R(t) = 1$ indicates the stability of the stationary soliton.

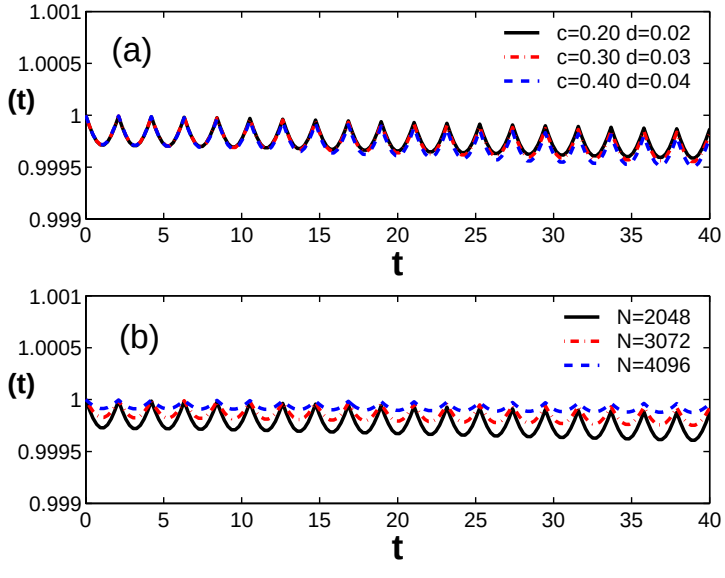


Fig. 3. (a) Normalized energy $R(t)$ versus time for three different higher-order parameters $c$ and $d$ while the other parameters are kept at the same values as in Figure 2. The energy evolution shows very small fluctuations (less than 0.03% in comparison to its initial value) as the magnitude of parameters monotonically increases. (b) The energy fluctuation does not originate from the breathing nature of the soliton but from the numerical grid size since it can be controlled by increasing the spatial grid points from $N = 2048$ to $N = 4096$ for the case of the plot with $c = 0.20$ and $d = 0.02$.

any curve of this figure represents a stationary soliton with defined width and peak amplitude. For the case of positive nonlinear parameters, i. e., $q = 1.0$, it is shown that the width of the soliton rapidly decreases and vanishes at $Q = p/(c+2d)$. However, for the case of a negative nonlinear parameter, the width of soliton increases as $Q$ increases and converges to a constant width as $Q >> p/(c+2d)$. In the other case, as shown in Fig. 1b, the width monotonically decreases as $Q$ increases for the case of $p = -0.5$ and $q = -1$.

Before full numerical simulations for verifying the stability of the stationary solitons, we numerically integrate the width parameter $f(t)$ in (6) with the initial conditions $f = 1$ and $\mathrm{d}f/\mathrm{d}t = 0$ at $t = 0$ for three values of $Q$ (0.01, 0.50, 1.30) and $r$ (7.06, 0.94, 0.51), respectively, while keeping the other parameters as $p = 0.50$, $q = 1.00$, $c = 0.10$, and $d = 0.01$, and find that $f(t)$ is invariant from its initial value, i. e., $f(t) = 1$. This stationarity property is verified for several other randomly chosen points on different curves of Figure 1.

To verify the predictions of the analytical results, which are based on the paraxial approximation [9, 10], we perform a numerical simulation of (1) adopting the widely used split-step Fourier method and take the Crank-Nicholson implicit scheme for time propagation under periodic boundary conditions [13, 14] with the initial profile provided by the width and peak constraint in (7). The numerical simulations are carried

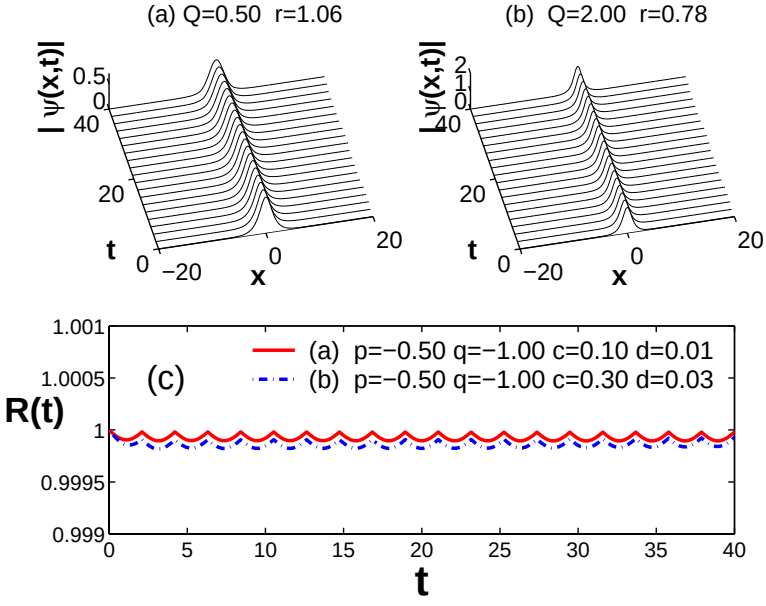


Fig. 4. (a, b) Numerically simulated propagations, with both the dispersion and nonlinear parameters being negative as indicated in (c), of stationary solitons with two different peak amplitudes and widths. The stability again confirms the validity of the analytic results. (c) Normalized energy $R(t)$ versus time. Stability of both stationary solitons is indicated for the case of spatial grid points $N = 4096$.

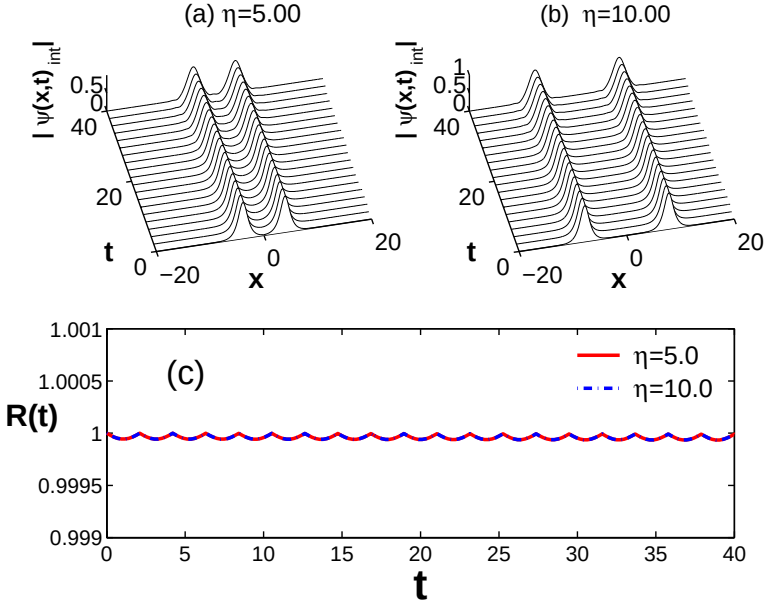


Fig. 5 (a, b) Numerically simulated propagations of two stationary solitons for two separation distances $\eta = 5$ and $\eta = 10.0$, respectively, with the parameters indicated in Figure 4b. (c) Normalized energy $R(t)$ versus time. Stability of both stationary solitons is indicated for the case of spatial grid points $N = 4096$.

out by varying the number of discrete Fourier modes between $N = 1024$ and $N = 4096$, and various time steps between $10^{-2}$ and $10^{-3}$. For the purpose of illustration, we choose the parameters as above, i. e., $p = 0.50$, $q = 1.00$, $c = 0.10$, $d = 0.01$, $Q = 0.50$, and $r = 0.94$. The results of the direct numerical simulations of (1) with these input parameters are also shown in Figure 2. The initial profile has a remarkable stability during its propagation as demonstrated in Fig. 2a for the modulus of amplitude and for its contour plot in Fig. 2b, respectively. Furthermore, in order to better understand the dynamical behaviour of the soliton, we calculate the total energy defined as $R(t) \equiv \int_{-\infty}^{+\infty} |\psi(x,t)|^2 \mathrm{d}x / \int_{-\infty}^{+\infty} |\psi(x,0)|^2 \mathrm{d}x$. Figure 2c shows the invariance of the initial energy $R(0)$, confirming the stability of the soliton. In order to understand the effect of the magnitude of the model parameters on the soliton dynamics, we performe the en-

ergy ratio calculation by increasing the magnitude of the higher-order terms in (1). According to Fig. 3a, the energy evolution shows only minor fluctuation (less than 0.03% in comparison to its initial value), as the magnitude of parameters monotonically increases, while using $N = 1024$ grid points. However, this energy fluctuation does not originate from the breathing nature of the soliton but from the numerical grid size since it can be controlled by increasing the spatial grid points from $N = 2048$ to $N = 4096$, as shown in Fig. 3b for the case of the plot with $c = 0.20$ and $d = 0.02$ in Figure 3a.

We now investigate the evolution of the stationary soliton in the case of both negative dispersion and nonlinearity parameters, i. e., $p = -0.5$ and $q = -1.0$, respectively, corresponding to those in Figure 1b. As clearly demonstrated in Figs. 4a and b for two sets of different model parameters (as shown in Fig. 4c) with two different peak amplitudes and widths, we still find that the initial pulse propagates very stably, confirming the assumption of the paraxial ray approximation. Similar to the case of a positive dispersion term, the energy fluctuation is negligible during its propagation regardless of the size of the parameters, as demonstrated for the case of $N = 4096$ spatial grid points in Figure 4c.

Finally, we now would like to understand the interaction dynamics of two stable solitons with an initial profile $\psi(x,0)_{\rm int} = \psi(x+\eta) + \psi(x-\eta)$, where $\eta$ is a separation between the waves. Figures 5a and b show, for examples, by using the same parameters as in Fig. 4b and $N = 4096$ grid points, the propagations of two initial profiles separated by $\eta = 5$ and $\eta = 10$, respectively. The presence of another stable soliton separated by a far distance does not influence the dynamics of an individual soliton and does not change the stability of the combined solitons as shown in Figure 5c. We have performed other simulations using other sets of the parameters to confirm that for $\eta \leq \eta_c \simeq 2.5$ the initial profiles overlap each other so that the combined wave does not show any stable propagation.

In conclusion, by adopting the paraxial ray approximation method [9, 10] used for finding spatial solitons in a photorefractive medium [11, 12], we have found the existence condition for the stationary solitons of the 1D MCGLE (1). We have identified the parameter space of the peak amplitude and pulse width for such stationary bright solitons. It has been numerically confirmed that the stationary bright solitons can exist regardless of the signs of the dispersion parameter $p$ and they propagate very stably, which confirms the analytical prediction based on the paraxial ray approximation. Even though, the analytic expression for multi-solitons has not been obtained, it has been numerically confirmed that the combined profiles also show the same stable stationary behaviour.

*Acknowledgements*

This work was supported by Catholic University of Daegu in 2007.

[1] I. S. Aranson and L. Kramer, Rev. Mod. Phys. **74**, 99 (2002).
[2] P. Kolodner, Phys. Rev. A **44**, 6448 (1991).
[3] M. Dennin, G. Ahlers, and D. S. Cannell, Phys. Rev. Lett. **77**, 2475 (1996).
[4] K. G. Müller, Phys. Rev. A **37**, 4836 (1988).
[5] Y. Kuramoto, Chemical Oscillations, Waves and Turbulence, Springer, Berlin 1984.
[6] A. Mohamadou, A. K. Jiotsa, and T. C. Kofané, Chaos, Solitons and Fractals **24**, 957 (2005).
[7] L. Smolin, Phys. Lett. A **113**, 408 (1986).
[8] E. Yomba and T. C. Kofané, Chaos, Solitons and Fractals **15**, 197 (2003).
[9] S. A. Akhmanov, A. P. Sukhorukov, and R. V. Khokhlov, Sov. Phys. USP **10**, 609 (1968); S. A. Akhmanov, A. P. Sukhorukov, and R. V. Khokhlov, in: Laser Handbook, Vol. II (Eds. A. T. Arechi, E. D. Shulz Dubois), North Holland, Amsterdam 1972, p. 1151.
[10] S. Konar and A. Sengupta, J. Opt. Soc. Am. B **11**, 1644 (1994).
[11] S. Jana and S. Konar, Phys. Lett. A **362**, 435 (2007).
[12] S. Jana and S. Konar, Opt. Commun. **273**, 324 (2007).
[13] J. A. C. Heideman and B. M. Herbst, SIAM J. Num. Ann. **23**, 485 (1986).
[14] W. P. Hong, Z. Naturforsch. **60a**, 719 (2005); **61a**, 23 (2006).